# Ammonia Stability in a Simulated Trace Contaminant Rich Cabin Environment

Matthew J. Kayatin<sup>1</sup> and Jay L. Perry<sup>2</sup>
NASA George C. Marshall Space Flight Center, Huntsville, AL, 35812, USA

The off-gassing of ammonia from hardware and metabolic sources presents a unique challenge to trace contaminant control system design, driving process flowrates to meet crewed air quality requirements. Accurately simulating representative trace contaminant cabin loads during ground testing is necessary to validate component design as well as understand potential contaminant propagation across life-support system process interface boundaries. This effort is complicated by the observed temporal concentration instability of gaseous ammonia in ground test chambers. To this end, ammonia concentration decay rates were characterized under controlled environmental conditions to better understand underlying phenomena and quantify incidental mass losses. The suspected chemical interaction between ammonia and trace acetaldehyde was investigated and its effect on species quantification was examined by both gas chromatography-mass spectrometry and Fourier-transform infrared spectroscopy. Recommendations for ground test procedures were made in order to best compensate for undesirable ammonia mass losses and mitigate test artifacts.

#### **Nomenclature**

C = concentration of ammonia

 $CH_4$  = methane

COTS = commercial-off-the-shelf

*DCM* = dichloromethane

ECLS = environmental control and life support FTIR = Fourier-transform infrared spectroscopy

 $g = \operatorname{gram}$ 

GC = gas chromatograph

GCMS = gas chromatography-mass spectrometry

*ISS* = International Space Station

L = liter

 $\lambda$  = decay constant

m = meter min = minute

*MSFC* = Marshall Space Flight Center

*NASA* = National Aeronautics and Space Administration

 $NH_3$  = ammonia

v = device flowrate (cubic meter/minute)

r218 = octafluoropropane

*RH* = relative humidity (percent)

s = second

SMAC = spacecraft maximum allowable concentration

t = time (minute)

TCC = trace contaminant control V = volume (cubic meter) Vchamber = vacuum chamber

*VOC* = volatile organic compound

<sup>&</sup>lt;sup>1</sup> Lead Engineer-Subsystems, ECLS Systems Development Branch, Space Systems Dept., NASA MSFC/ES62.

<sup>&</sup>lt;sup>2</sup> Technical Assistant, ECLS Systems Development Branch, Space Systems Dept., NASA MSFC/ES62.

# I. Introduction

Ammonia (NH<sub>3</sub>) present in a crewed spacecraft cabin environment is generated from hardware off-gassing and human metabolic processes. Historically, ammonia production rates were derived from Spacelab program data combined with published human metabolic studies, which then served as a basis for designing air quality controls aboard the International Space Station (ISS).<sup>1</sup> According to the 2009 proposed working cabin load model for trace contaminant control (TCC) system design, the primary ammonia source aboard a crewed spacecraft is human metabolism.<sup>2</sup> Note that in this load model, the metabolic component of the ammonia generation rate of 50 mg/personday is substantially larger than the equipment off-gassing rate of 8.5 × 10<sup>-5</sup> mg/kg-day. For perspective, the 2009 load model suggests that ammonia's contribution to the total metabolic off-gassing load of 10.7% is only second to that of methane.<sup>2</sup> Ammonia produced via metabolic pathways is liberated through the breath, sweat, and skin; of these metabolic pathways, ammonia is primarily liberated from human sweat and is thus dependent on sweat production rates which are elevated during exercise.<sup>3</sup>

#### A. Literature Survey on Metabolic Ammonia Sources

An updated literature survey was completed which adds additional references to the data set analyzed in 2009.<sup>2</sup> Results of the literature review indicate 48.6 mg/person-day to be an appropriate total metabolic liberation rate, which is consistent with the previously proposed rate magnitude. Specific findings pertaining to ammonia contributions from skin, sweat, and breath from the updated literature survey are presented in the following summary.

The sweat liberation component was found to contribute up to 27.3 mg/person-day or approximately 56% of the total daily load. This contribution is based on the 95% confidence interval upper bound for the ammonia concentration in sweat of 0.141 mg/mL identified by literature survey. This concentration is applied to a time averaged daily sweat production rate of 25.8 mL/minute<sup>8, 12-17</sup> during exercise periods lasting up to two hours and 0.6 mL/minute<sup>18, 19</sup> for normal activities up to 22 hours duration. The literature surveyed also indicates that sweat pH is 6.9 for the 95% confidence interval upper bound. At this pH, only 0.006% of the ammonia is expected to be available as free gas. Conservatively, it is assumed that 5% of the ammonia in sweat is available as free gas to account for the higher end of the reported sweat pH range.

The ammonia source component attributed to breath accounts for 8.7 mg/person-day or approximately 18% of the total daily load. This load component is based on the 95% confidence interval upper bound for the ammonia concentration in breath of 0.79 mg/m $^3$ . This concentration is applied to a time averaged breath volume rate of 0.46 m $^3$ /h. $^{33-36}$ 

The final release pathway for metabolically-produced ammonia is via the skin. Ammonia liberation from the skin was found to contribute 12.6 mg/person-day<sup>37</sup> and this quantity is approximately 26% of the total daily ammonia load.

# **B.** Trace Contaminant Control Design and Test Considerations

From the perspective of cabin air quality with respect to crew health, ammonia is of greater concern due to the juxtaposition of its relatively large production rate and low 180-day spacecraft maximum allowable concentration (SMAC) of 2 mg/m<sup>3</sup>.<sup>38</sup> In fact, the coupling of the NH<sub>3</sub> generation rate and SMAC specified the process flowrate requirement for the ISS TCC system charcoal bed. The ISS TCC charcoal bed assembly utilizes phosphoric acid-treated charcoal to control ammonia by chemisorption.<sup>2</sup> Future exploration TCC system architectures will be subjected to similar process design constraints. Efforts are currently underway to aid in process design and equipment sizing by modeling ammonia adsorption on candidate acid-treated charcoal.<sup>39, 40</sup>

Exploration hardware prototypes and dynamic adsorption models will need to be proven and anchored by a rigorous ground test program. Accurately simulating representative trace contaminant cabin loads in ground testing has proven to be challenging historically due to the apparent temporal concentration instability of ammonia gas, even in quiescent environments. These instabilities were hypothesized to be from surface passivation and/or interactions with volatile organic compounds (VOC) representative of nominal cabin loads. It is necessary to overcome and/or better understand these instabilities in order to accurately measure TCC system performance as well as understand potential contaminant propagation across life-support system process interface boundaries.

# **II.** Experimental Chamber Test Methods

Testing was performed in the MSFC Vacuum Chamber (Vchamber), a 96.3 m<sup>3</sup> vessel located in building 4755. The Vchamber is a sealed mixing chamber ideally suited for simulating a stable environment of trace contaminants. Mixing is provided by commercial-off-the-shelf (COTS) ventilation fans, humidification by a COTS moisture wicking

humidifier, and dehumidification by a COTS unit capable of continuous operation. Chamber humidity was monitored using a Sable Systems RH-300 sensor and tests were performed under ambient temperature and pressure.

Ammonia was injected by pumping from a 10 L Tedlar® gas bag filled with a certified blend of  $1.3 \text{ vol.} \% \text{ NH}_3$  in air purchased from Airgas. Each 10 L bag provides  $\approx 98.8 \text{ mg}$  of  $NH_3$  which is diluted to  $\approx 1 \text{ mg/m}^3$  by the chamber volume. Octafluoropropane (r218) was injected by pumping from a 10 L Tedlar® gas bag filled with a blend of 10 vol. % r218 in air. Each 10 L bag provides  $\approx 8.39 \text{ g}$  of r218 which is diluted to  $87 \text{ mg/m}^3$  by the chamber volume. Methane (CH<sub>4</sub>) was injected by pumping from a 1 L Tedlar® gas bag filled with pure CH<sub>4</sub>. Each 1 L bag provides  $\approx 662 \text{ mg}$  of CH<sub>4</sub> which is diluted to  $\approx 6.9 \text{ mg/m}^3$  by the chamber volume. Both r218 and CH<sub>4</sub> were purchased from Sexton. VOC injections were made manually by pre-measured aliquot evaporations from sample vials on a warm hotplate. Aliquots were calculated based on the combination of desired mg/m³ concentrations, chamber volume, and pure component liquid density. All pure VOC liquids were purchased in the highest grade available from Sigma-Aldrich.

Quantification and VOC analysis was performed by gas chromatography-mass spectrometry (GCMS) with an Agilent 7890 capillary gas chromatograph (GC) utilizing a single analytical column [Restek Rxi-624Sil MS (20 m x 0.18 mm x 1.0 µm)] equipped with both a flame ionization and mass selective detector. A Gerstel TDSG thermal desorption system provided trapping of contaminants within a layered sorbent tube followed by cryogenic (-120°C) focusing on quartz glass wool at the GC inlet. Sample flows were metered using an integrated mass flow controller. Calibrations were made using gas phase standards generated via National Institute for Standards and Technology traceable permeation tubes heated within a Kin-Tek gas generator and regulated by a Kin-Tek Interface Module. Calibrations were referenced to the flame ionization detector whereas the mass selective detector was utilized for identification of chemical unknowns and reaction byproducts. Samples were drawn from the test chamber in a closed loop utilizing an external sample pump and instrument sample flow was provided via slip stream to the GC and returned via the Gerstel sampling loop to the chamber to avoid any mass losses.

Ammonia, CH<sub>4</sub>, and r218 quantification was performed with a Gasmet DX4040 Fourier-transform Infrared (FTIR) spectrometer. The FTIR features a Peltier-cooled mercury cadmium telluride detector with interferometer having 8 cm<sup>-1</sup> resolution. Long measuring times of 5 minutes (min) through a 9.8 m optical path length cell allow for trace gas detection. The FTIR operated on an independent, closed loop with the chamber and sample flow was provided by an internal pump which automatically operated intermittently between measurements.

## III. Results & Discussion

Ammonia stability was examined by monitoring chamber concentrations over time. The influence of environmental effects and trace contaminants were studied to better understand underlying ammonia concentration decay rate phenomena. From these observations, a rational ground testing strategy to accurately simulate trace contaminant rich environments in the presence of ammonia was proposed.

#### A. Chamber Atmosphere Stability

The temporal concentration instability of three serial ammonia injections is shown by Fig. 1. Each injection exhibited a peak concentration maximum followed by a rapid decay in observed chamber ammonia concentration.

This behavior is unlike that of most trace contaminants where stable chamber VOC concentrations are typically observed over a period of days. The observed NH<sub>3</sub> concentration decay is a challenge for ground hardware testing where targeted plateau concentrations are desired to challenge processes with representative spacecraft cabin conditions. Furthermore, the temporal losses skew or mask the true cabin mass balance. To better understand the origin and rate of the concentration decay, test data for each individual injection was regressed against physical and mathematical models.

Exponential decay is described by the differential equation shown by Equation 1 wherein the concentration of ammonia (C) decreases at a constant rate according to the decay constant ( $\lambda$ ). The solution to Equation 1 is shown by Equation 2. Using the method of least squares, the initial peak chamber concentration  $C_0$ 

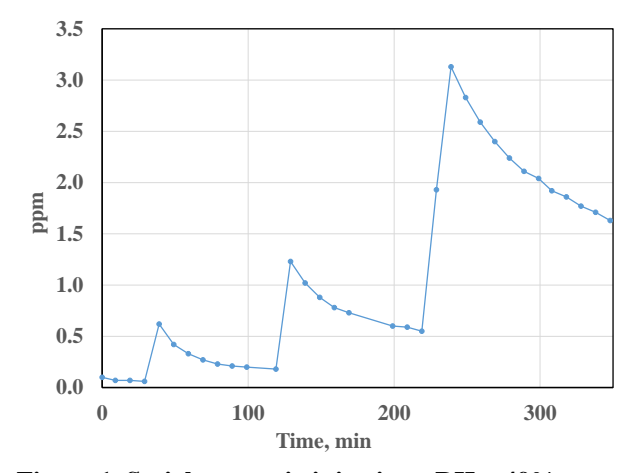


Figure 1. Serial ammonia injections. RH = 49%.

and  $\lambda$  may be determined from test data, where  $\lambda$  has units of inverse seconds (s). While the value of  $\lambda$  is useful for comparing decay rates between injections with varied initial chamber peak concentrations and environmental conditions, it lacks physical meaning. Equation 3 introduces the mass balance for a cabin of known volume (V) interacting with a removal device having a flow rate (v), where v has units of  $m^3/min$ . By comparison of Equations 1 and 3, a relationship between  $\lambda$  and v can be made and the value of v easily determined from the regression parameters. Determining the value of v is valuable for ground test planning as the expected incidental rate of mass loss due to temporal concentration instability can be estimated and factored into the desired test plan ammonia injection rate, as required to simulate metabolic loads.

$$\frac{dC}{dt} = -\lambda C \tag{1}$$

$$C(t) = C_0 e^{-\lambda t} \tag{2}$$

$$\frac{dC}{dt} = -\frac{vC}{V} \tag{3}$$

Figure 2 displays the measured ammonia concentration trends from Fig. 1 (closed symbols) overlaid with an exponential regression curve as well as the mass balance model (open symbols) as described by Eq. 3, wherein the value of  $\nu$  was found using  $\lambda$ . Table 1 summarizes the peak initial ammonia concentration for each injection,

determined regression parameters, and resulting effective removal device flow. Note that the measured decay rates and simulated removal device flow decrease with increasing initial chamber spike mass. For reference to nominal ISS ammonia loads of approximately 0.13 mg/m³, we can conservatively estimate the incidental mass loss at this concentration to be 0.21 mg/min.

The functional form of Equation 2 may also be representative of the rate law for a first order chemical reaction mechanism wherein  $\lambda$  represents the rate constant k. The apparent dependence on the observed decay rates on initial ammonia concentration,

Table 1. Regression and model parameters. \*From experimental test data.

$C_0*$	$C_0$	λ	ν
$mg/m^3$	$mg/m^3$	$s^{-1}$	m <sup>3</sup> /min
0.43	0.35	0.0165	1.59
0.86	0.80	0.0114	1.09
2.18	2.01	0.0056	0.54

combined with the lack of self-similarity in k, likely indicates that ammonia instability is not the result of a simple chemical degradation in this case.

#### **B.** Environmental Effects on Stability

The effect of the chamber relative humidity (RH) and influence of the mixing fans was of interest to better understand the observed decay rates. Ammonia injection into an unmixed atmosphere is shown by Fig. 3a where a peak concentration of 1.36 ppm appears to stand out from the data trend showing that the chamber is not well mixed within the first 10 min of the test. Including this data point into the regression shown by Fig. 3b resulted in a poor fit, as expected. Thus, this data point was excluded from the regression as it would not properly represent the decay rate of a quiescent atmosphere. Parameters extracted from Fig. 3b were  $C_0 = 0.61 \text{ mg/m}^3$  and  $\lambda = 0.0029 \text{ s}^{-1}$  which resulted in determining v = 0.28 m<sup>3</sup>/min at 45% RH. Based on the parameters previously extracted from ammonia concentration decay in the presence of chamber ventilation fans (Table 1), there appears to be a noticeable reduction in decay rate. This result may indicate that adsorption to chamber surfaces, enhanced by the forced convective mixing of the ventilation fans, contributes to the observed ammonia concentration instability. To examine the role of chamber mixing on ammonia concentration decay, as well as examine the influence of chamber humidity, experiments were conducted at 23% relative humidity. Concentration decay behavior having a shape consistent with previous observations was seen for an injection characterized by  $C_0 = 0.53 \text{ mg/m}^3 \text{ and } \lambda = 0.0088 \text{ s}^{-1} \text{ (v} = 0.84 \text{ m}^3/\text{min)}$ . Again, based on the parameters previously extracted from ammonia concentration decay in the presence of chamber ventilation fans (Table 1), there appears to be a noticeable reduction in decay rate at this lower humidity. Disabling the ventilation fans at lower relative humidity further delayed the decay rate towards 0.001 - 0.0008 s<sup>-1</sup> depending on whether the unmixed injection spike was included into the regression or not. Thus, we confirm that forced convection does increase observed ammonia concentration decay rates and it appears this effect may be amplified by the presence of humidity. Neither of these factors are parameters that would be controlled to mitigate the effect of ammonia concentration decay since both atmospheric mixing and comfortable atmospheric humidity are required for spaceflight, and thus, ground testing.

### C. Effect of Trace Contaminants

A stable atmosphere of trace contaminants representative of typical cabin loads and a wide array of common compound classes was simulated by injection into the Vchamber. Compound classes represented included alcohols, aldehydes, aliphatic and aromatic hydrocarbons, chlorinated hydrocarbons [dichloromethane (DCM)], ketones, fluorocarbons, and siloxanes [hexamethylcyclotrisiloxane, i.e. D3]. Ammonia was injected into this atmosphere to

(a) Data Mass Balance ---- Expon. (Data) 0.5  $y = 0.3507e^{-0.0165x}$  $R^2 = 0.9149$ 0.4 0.3 0.2 0.1 0.00 20 40 60 80 Time, min (b) Data Mass Balance Expon. (Data) 1.0  $y = 0.7988e^{-0.0114x}$  $R^2 = 0.9671$ 0.8 0.6  $mg/m^3$ 0.2 0.0 20 40 60 80 0 Time, min (c) Data Mass Balance Expon. (Data) 2.5  $y = 2.0358e^{-0.0056x}$  $R^2 = 0.9724$ 2.0 1.5 mg/m<sup>3</sup> 0.5 0.0 0 20 40 60 80 100 120 Time, min

Figure 2. Regression of ammonia datasets for peak concentrations a)  $0.43~\text{mg/m}^3$ , b)  $0.86~\text{mg/m}^3$ , and c)  $2.34~\text{mg/m}^3$ .

observe the temporal concentration stability in a representative cabin environment as shown by Fig. 4. Two 10 L injections were made with a peak concentration of 1.4 ppm and 2.0 ppm, respectively. After each NH3 injection, a significant and unexpected increase acetaldehyde concentration was measured by GCMS. This is noteworthy because NH<sub>3</sub> is not typically detected by GCMS as a pure component, indicating a potential chemical interaction and/or coelution through the chromatograph. Fig. 5 displays the measured acetaldehyde background concentration by GCMS during serial pure ammonia injections. Ammonia concentration measurements were made by FTIR acetaldehyde concentrations were on the order of 10 parts per billion throughout confirming that pure ammonia does not elute from chromatograph over the same retention time window. This finding should preclude false positives for acetaldehyde due to pure ammonia elution.

FTIR spectra collected on ammonia and acetaldehyde atmospheres were scrutinized for evidence of non-covalent interactions via red or blue shifting to the extent possible by the instrument resolution. Kayatin (2012) has previously shown this analysis beneficial for probing non-covalent polymer-solvent interactions to elucidate hydrogen bonding.41 Unlike condensed-phase spectra, where sample media are much more concentrated, the spectra of trace gas atmospheres are missing the richness and clear definition of many expected peak vibrations. Fig. 6a shows the FTIR fingerprint region highlighting the peak at 965 cm<sup>-1</sup>. This peak was attributed to a deformation mode of ammonia and its concentration directly scales with absorbance as shown by the inset.<sup>42</sup> We interpret the absence of any non-linear behavior to be evidence against a gas-phase chemical interaction between species. Furthermore, no apparent mid-infrared spectral shifts were observed for the experiments discussed herein. This may be a result of the low (8 cm<sup>-1</sup>) spectral resolution provided by the FTIR, however. To further investigate potential physicochemical interactions (indirectly), the influence of acetaldehyde introduction ammonia concentration decay trends/rates was examined.

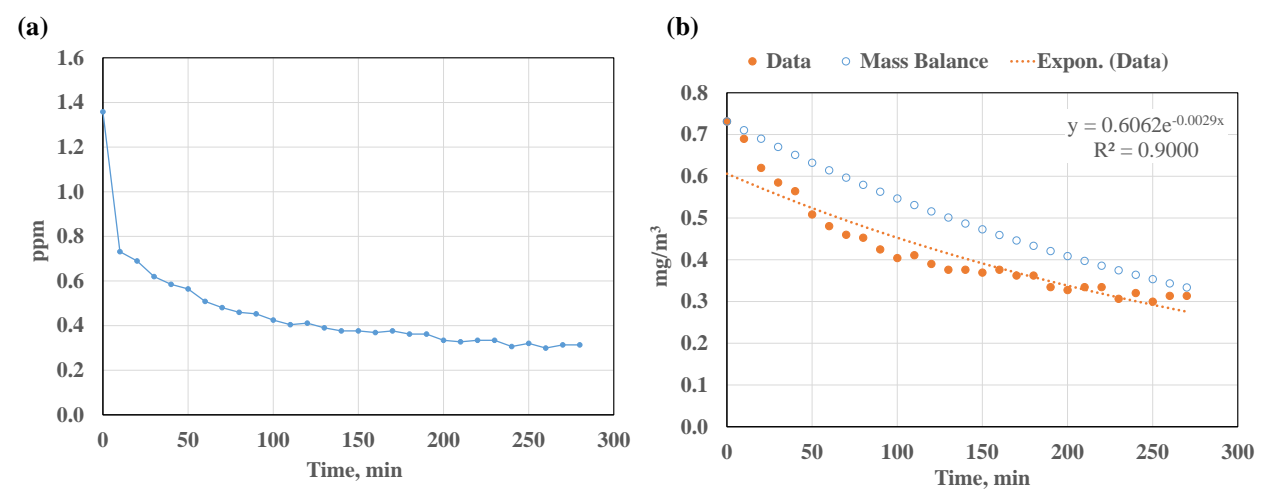


Figure 4. a) Injection into an unmixed chamber and b) regression of unmixed dataset excluding the  $1^{st}$  data point. RH = 45%.

Since we have shown that pure ammonia is unstable in a clean test chamber over time, experiments to detect any changes in the expected concentration decay rate of ammonia upon acetaldehyde introduction, and vice versa, were also performed. After first establishing a stable mean acetaldehyde concentration of 1.85 ppm (7.25 mmol), 30 L of ammonia was dosed to bring its concentration to 3.4 ppm (13.3 mmol). For reference, this atmosphere represents a peak ammonia to acetaldehyde molar ratio of 1.83 and the chamber RH was 37% at this time. Acetaldehyde concentration as measured by GCMS rose to  $\approx 2.5$  ppm, which is in error based on the starting load of acetaldehyde dosed into a clean chamber atmosphere. The decay rate was well-behaved ( $R^2 = 0.98$ ), and consistent with similar regression parameters as those shown by Table 1, having  $C_0 = 2.29$  mg/m³ and  $\lambda = 0.0075$  s<sup>-1</sup> which resulted in determining v = 0.73 m³/min. In the opposite order, an ammonia rich atmosphere was established with a peak load of 3.4 ppm (13.3 mmol) into which  $\approx 10.7$  mmol of acetaldehyde was added. Due to the potential interactions or error

introduced to the GCMS measurement, the exact recovery of acetaldehyde into the atmosphere was unknown theoretical peak concentration was 2.7 ppm (4.9 mg/m<sup>3</sup>). For reference, this corresponds to a peak ammonia to acetaldehyde molar ratio of 0.82 and the chamber RH was 39% at this time. The observed ammonia concentration decay rate was well-behaved  $(R^2 = 0.95)$ , and consistent with a similar regression parameters as those shown by Table 1, having  $C_0 = 2.05 \text{ mg/m}^3 \text{ and } \lambda =$  $0.0052 \text{ s}^{-1}$  which resulted in determining v =0.50 m<sup>3</sup>/min. It is also noteworthy that no interruption or inflection was observed to the already in progress concentration decay rate of ammonia as shown by Fig. 6b. This observation does not support a gas-phase reaction of ammonia and acetaldehyde. After decaying to 0.99 ppm NH<sub>3</sub>, second

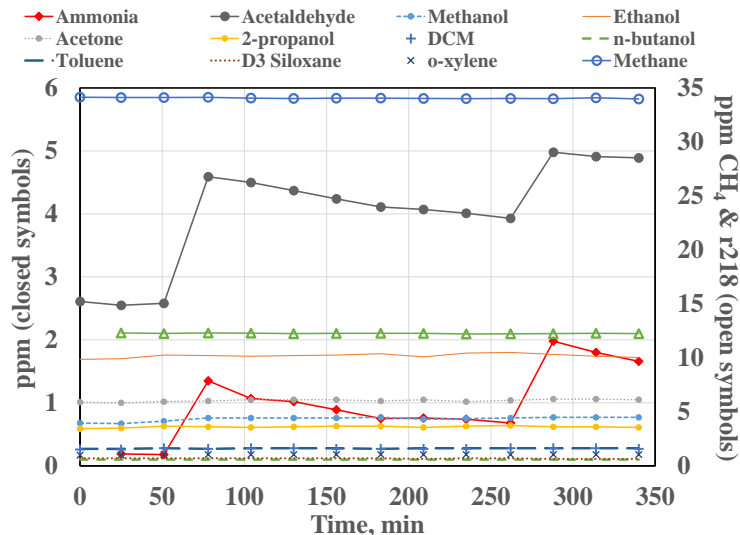


Figure 3. Stability of VOC classes and ammonia. NH<sub>3</sub>, CH<sub>4</sub>, and r218 measured by FTIR. VOC measured by GCMS. RH = 37%.

injection of ammonia was also added, peaking at 1.95 ppm (7.6 mmol). Likewise, the decay rate was well-behaved ( $R^2 = 0.99$ ) having  $C_0 = 1.89$  mg/m³ and  $\lambda = 0.0032$  s<sup>-1</sup> which resulted in determining  $\nu = 0.31$  m³/min. Thus, the effort to elucidate any indirect insight into ammonia-acetaldehyde potential interactions via observed decay rate kinetics was unremarkable at these concentrations.

In absence of compelling evidence supporting gas-phase physicochemical interactions, we searched the literature for further resolution. Condensation reactions between acetaldehyde and ammonia have been reported in the aqueous

phase, including the formation of a cyclic trimer.<sup>43, 44</sup> No reference was available extending these reactions to the gas phase at room temperature, however. Interestingly, this reaction is of interest to researchers studying the interstellar

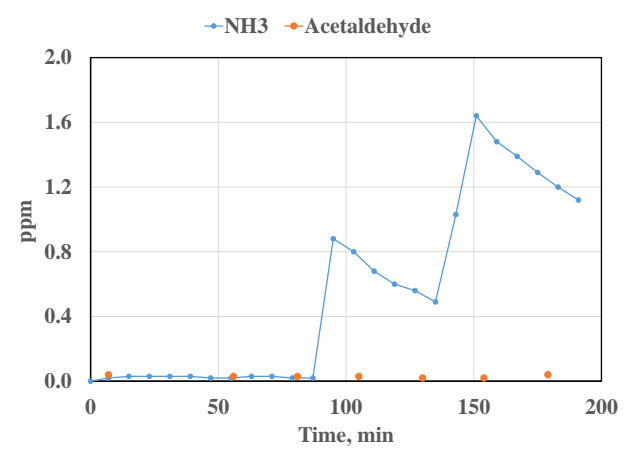


Figure 5. Measured acetaldehyde concentration by GCMS during ammonia injection. RH = 22%.

chemistry of cold ices and various interstellar media. Duvernay et al. (2010) deposited pure component ices of ammonia and acetaldehyde and found them to react to form alpha-aminoethanol at 130 K (-134°C).<sup>45</sup> Vinogradoff et al. (2012) also found that at cryogenic conditions (near 160 K or -113°C) the trimer is formed in these ices in the presence of formic acid. 46 These solid reactions occur at cryogenic conditions remarkably similar to those found within the GC cryofocusing step, where both trace contaminants and moisture are condensed together at 153 K (-120°C) and subsequently warmed to desorb on the capillary column for separation. Thus, we believe we have a plausible source of ammonia-acetaldehyde interaction and the resulting measurement artifact. The exact cause for the resulting amplification of acetaldehyde peak areas remains elusive presently and is beyond the scope of this work. We note that scrutiny of mass spectra shows

only evidence of pure acetaldehyde, however, which may indicate thermal degradation of any cryogenic reaction product reverts back to pure components.

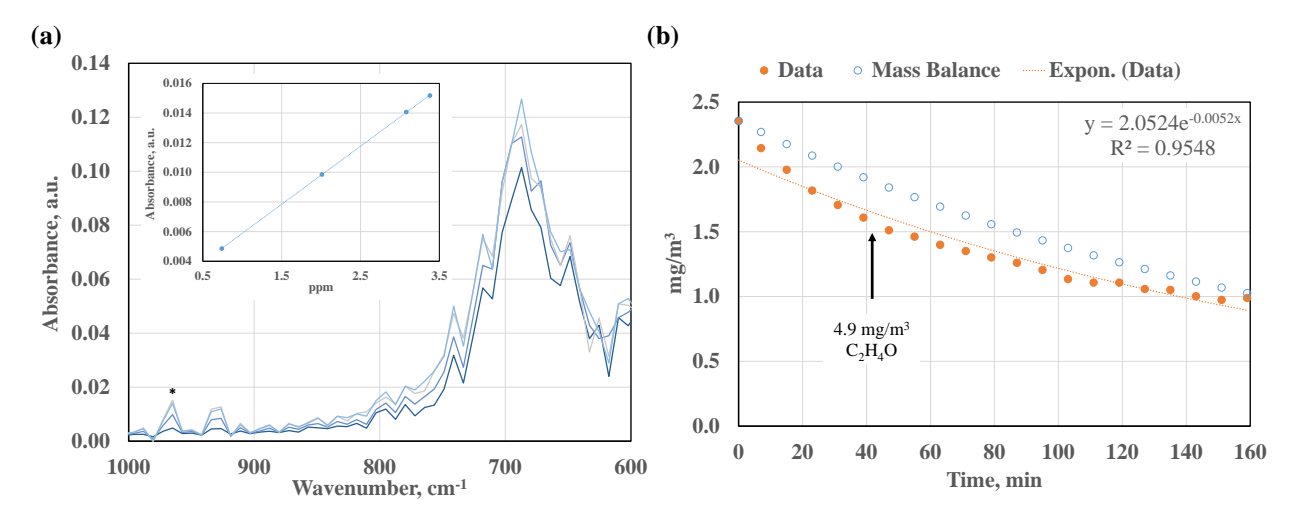


Figure 6. a) FTIR spectra of ammonia rich atmosphere in presence of acetaldehyde. RH = 39%. Inset: Peak absorbance vs. concentration at 965 cm<sup>-1</sup>. b) Acetaldehyde (C<sub>2</sub>H<sub>4</sub>O) dosed into an ammonia rich atmosphere.

# **D.** Ground Test Strategy

Due to the observed temporal concentration instability of ammonia, desired chamber ammonia injection rates must be augmented at anticipated mass loss rates. For example, previous testing conducted by NASA Advanced Exploration Systems under the Atmosphere Resource Recovery and Environmental Monitoring Project specified ammonia injection rates of 7.1 mg/h to adequately simulate ISS cabin generation rates.<sup>47</sup> Based on test data presented herein, at targeted relevant chamber concentrations, we estimate additional losses on the order of 10 mg/h. These adsorptive losses can be categorized as an additional incidental mass loss route.<sup>48</sup> Towards specification of a functional NH<sub>3</sub> injection system, a targeted rate of 20 mg/h was selected. Calculations show that feeding a ruggedized 100 mL/min mass flow controller from a gas cylinder of 1 vol. % NH<sub>3</sub> will afford an injection rate range from approximately 2.3 mg/h up to 45.6 mg/h, allowing margin to accommodate additional losses. Since the exact mass accountability is

difficult to ascertain, NH<sub>3</sub> should be injected continuously while actively monitoring a sample port immediately upstream of the primary TCC process of interest using FTIR.

An interaction of ammonia and acetaldehyde is suspected based on the observed amplification of measured acetaldehyde concentrations and lack of apparent artifact while analyzing gas streams containing only the pure components by GCMS. In order to avoid skewing test data, we propose substituting the acetaldehyde load with an analog of similar molar volume. This can be achieved by substituting the desired acetaldehyde injection rate with additional methanol. Trace contaminant breakthrough test data on shallow depth charcoal beds have shown neither acetaldehyde nor methanol are well controlled by high velocity adsorption.<sup>49</sup> In addition, test data on a high aspect ratio bed showed remarkably similar breakthrough trends between compounds.<sup>48</sup> Thus, substitution with an additional methanol load will not impact measured outcomes of charcoal bed performance. Furthermore, the full load will still reach the TCC catalytic oxidizer and assuming that there is no discrepancy between each compound's thermal oxidation efficiency, this substitution should not impact measured test performance.

#### IV. Conclusion

The temporal concentration instability of ammonia injected into a ground test chamber was shown and characterized by regression against mathematical and physical models. Test results indicate that adsorption to chamber surfaces, enhanced by forced convection, contributes to the observed ammonia instability and this effect is enhanced in presence of humidity. While most common classes of trace chemical contaminants do not interact or influence the ammonia concentration decay rate, the presence of acetaldehyde introduces an artifact into the aldehyde measurement as determined by GCMS. To overcome the observed instability of ammonia for ground testing we recommend continuous injection and monitoring upstream of process equipment of interest. To overcome introducing experimental artifacts resulting from the apparent cryogenic incompatibility of ammonia and acetaldehyde we recommend substituting acetaldehyde's mass load with additional methanol mass.

# Acknowledgments

The authors acknowledge the AES Life Support Systems project for funding and Kenny Bodkin for chamber infrastructure improvements.

## References

<sup>1</sup>Perry, J. L., "Trace Chemical Contaminant Generation Rates for Spacecraft Contamination Control System Design," NASA TM-108497, 1995.

<sup>2</sup>Perry, J. L. "A Design Basis for Spacecraft Cabin Trace Contaminant Control," *SAE International Journal of Aerospace*, Vol. 4, No. 2009-01-2592, 2009, pp. 584-591.

<sup>3</sup>Perry, J. L., "Elements of Spacecraft Cabin Air Quality Control Design," NASA TP-207978, 1998.

<sup>4</sup>Brusilow, S.W. and Gordes, E.H., "Ammonia Secretion in Sweat," *American Journal of Physiology*, Vol. 214, No. 3, 1968, pp. 513-517.

<sup>5</sup>Itoh, S. and Nakayama, T., "Ammonia in Human Sweat and Its Origin," *Japanese Journal of Physiology*, Vol. 3, 1952, pp. 133-137.

<sup>6</sup>Robinson, S. and Robinson, A.H., "Chemical Composition of Sweat," *Physiological Reviews*, Vol. 34, No. 2, 1954, pp. 202-220.

<sup>7</sup>Adams, R., Johnson, R.E., and Sargent, F., "The Osmotic Pressure (Freezing Point) of Human Sweat in Relation to Its Chemical Composition," *Q J Exp Physiol Cogn Med Sci*, Vol. 43, No. 3, 1958, pp. 241-257.

<sup>8</sup>Czarnowski, D. and Gorski, J., "Sweat Ammonia Excretion During Submaximal Cycling Exercise," *Journal of Applied Physiology*, Vol. 70, No. 1, 1991, pp. 371-374.

<sup>9</sup>Alexiou, D., Anagnostopoulos, A., and Papadatos, C., "Total Free Amino Acids, Ammonia, and Protein in the Sweat of Children," *The American Journal of Clinical Nutrition*, Vol. 32, No. 4, 1979, pp. 750-752.

<sup>10</sup>Meyer, F., Laitano, O., Bar-Or, O., McDougall, D., and Heingenhauser, G.J.F., "Effect of Age and Gender on Sweat Lactate and Ammonia Concentrations During Exercise in the Heat," *Brazilian Journal of Medical and Biological Research*, Vol. 40, No. 1, 2007, pp. 135-143.

<sup>11</sup>Schmidt, F.M., Vaittinen, O., Metsälä, J., Lehto, M., Forsblom, C., Groop, P.H., and Halonen, L., "Ammonia in Breath and Emitted from Skin," *Journal of Breath Research*, Vol. 7, No. 1, 2013, p. 017109.

<sup>12</sup>Patterson, M.J., Galloway, S.D., and Nimmo, M.A., "Variations in Regional Sweat Composition in Normal Human Males," *Experimental Physiology*, Vol. 85, No. 6, 2000, pp. 869-875.

<sup>13</sup>Green, J.M., Pritchett, R.C., Tucker, D.C., Crews, T.R., and McLester, J.R., "Sweat Lactate Response during Cycling at 30 C and 18 C WBGT," *Journal of Sports Sciences*, Vol. 22, No. 4, 2004, pp. 321-327.

<sup>14</sup>How Much Do Athletes Sweat? Australian Institute of Sport, Department of Sports Nutrition, 2004.

- <sup>15</sup>Greenhaff, P.L. and Clough, P.J., "Predictors of Sweat Loss in Man during Prolonged Exercise," *European Journal of Applied Physiology*, Vol. 58, No. 4, 1989, pp. 348-352.
- <sup>16</sup>Burry, J.S. Evans, R.L., Rawlings, A.V., and Shiu, J., "The Effect of Antiperspirants on Whole Body Sweat Rate and Thermoregulation," *International Journal of Cosmetic Science*, Vol. 25, No. 4, 2003, pp. 189-192.
- <sup>17</sup>Shirreffs, S.M., Aragon-Vargas, L.F., Chamorro, M., Maughan, R.J., Serratosa, L., and Zachwieja, J.J., "The Sweating Response of Elite Professional Soccer Players to Training in the Heat," *International Journal of Sports Medicine*, Vol. 26, No. 2, 2005, pp. 90-95.
- <sup>18</sup>Webb, P, (ed.), "Bioastronautics Data Book," NASA SP-3006, National Aeronautics and Space Administration, Washington, DC, 1964, pp. 224-225.
- <sup>19</sup>Wydevan, T. and Golub, M.A., "Generation Rates and Chemical Compositions of Waste Streams in a Typical Crewed Space Habitat," NASA TM 102799, NASA Ames Research Center, Moffett Field, California, August 1990, pp. 5-6.
- <sup>20</sup>Smith, D., Turner, C, and Spanel, P., "Volatile Metabolites in the Exhaled Breath of Healthy Volunteers: Their Levels and Distributions," *Journal of Breath Research*, Vol. 1, No. 1, 2007, p. 014004.
- <sup>21</sup>Brooks, S.M., Haight, R.R., and Gordon, R.L., "Age Does Not Affect Airway pH and Ammonia as Determined by Exhaled Breath Measurements," *Lung*, Vol. 184, No. 4, 2006, pp. 195-200.
- <sup>22</sup>Androver, R., Cocozzella, D., Ridruejo, E., Garcia, A., Rome, J., and Podesta, J.J., "Breath-Ammonia Testing of Healthy Subjects and Patients with Cirrhosis," *Digestive Diseases and Sciences*, Vol. 57, No. 1, 2012, pp. 189-195.
- <sup>23</sup>Solga, S.F., Mudalel, M.L., Spacek, L.A., and Risby, T.H., "Fast and Accurate Exhaled Breath Ammonia Measurement," *Journal of Visualized Experiments*, Vol. 88, 2014, p. e51658.
- <sup>24</sup>Spacek, L.A., Strzepka, A., Saha, S., Kotula, J., Gelb, J., Guilmain, s., Risby, T., and Solga, S.F., "Repeated Measures of Blood and Breath Ammonia in Response to Control, Moderate and High Protein Dose in Healthy Men," *Scientific Reports*, Vol. 8, No. 1, 2018, p. 2554.
- <sup>25</sup>Tsuboi, O, Momose, S., and Takasu, R., "Mobile Sensor that Quickly and Selectively Measures Ammonia Gas Components in Breath," *Fujitsu Sci. Tech. J.*, Vol. 53, Feb. 2017, pp. 38-43.
- <sup>26</sup>Spanel, P., Dryahina, K., and Smith, D., "Acetone, Ammonia and Hydrogen Cyanide in Exhaled Breath of Several Volunteers Aged 4-83 Years," *Journal of breath research*, Vol. 1, No. 1, 2007, p. 011001.
- <sup>27</sup>Nefedov, Y., Zaloguev, S.N., and Savina, V.P., "The Problem of Habitability in Spaceships," *Proceedings of the XXIV*<sup>th</sup> *International Astronautical Congress*, Baku, USSR, October 13, 1973, p. 207.
- <sup>28</sup>Turner, C., Spanel, P., and Smith, D., "A Longitudinal Study of Ammonia, Acetone and Propanol in the Exhaled Breath of 30 Subjects using Ion Flow Tube Mass Spectrometry," SIFT-MS, *Physiological Measurement*, Vol. 27, No. 4, 2006, pp. 321-337.
- <sup>29</sup>Mathew, T.L., Pownraj, P., Abdulla, S., and Pullithadathil, B., 'Technologies for Clinical Diagnosis Using Expired Human Breath Analysis,' *Diagnostics*, Vol. 5, No. 1, 2015, pp. 27-60.
- <sup>30</sup>Diskin, A.M., Spanel, P., and Smith, D., "Time Variation of Ammonia, Acetone, Isoprene, and Ethanol in Breath: A Quantitative SIFT-MS Study Over 30 Days," *Physiological Measurement*, Vol. 24, No. 1, 2003, pp. 107-119.
- <sup>31</sup>Hibbard, T., and Killard, A.J., "Breath Ammonia Analysis: Clinical Application and Measurement," *Critical Reviews in Analytical Chemistry*, Vol. 41, No. 1, 2011, pp. 21-35.
- <sup>32</sup>Kustov, V.V., and Tiunov, L.A., "Problems of Space Biology, Volume 11 The Toxicology of Products of Vital Activity and Their Importance in the Formation of Artificial Atmospheres of Hermetically Sealed Chambers," *NASA Technical Translation TT*, F-634, March 1971, p. 80.
- <sup>33</sup>Krieger, J., Maglasiu, N., Sforza, E., and Kurtz, D., "Breathing During Sleep in Normal Middle-Aged Subjects," *Sleep*, Vol. 13, No. 2, 1990, pp. 143-154.
- <sup>34</sup>Webb, P, (ed.), "Bioastronautics Data Book," NASA SP-3006, National Aeronautics and Space Administration, Washington, DC, 1964, p. 278.
- <sup>35</sup>De Castro, R., Lima, S., Sales, A., and Nobrega, A. "Minute-Ventilation Variability during Cardiopulmonary Exercise Test is Higher in Sedentary Man Than in Athletes," *Arquivos Brasileiros de Cardiologia*, Vol. 109, No. 3, Sept. 2017, pp. 185-190.
- <sup>36</sup>Segizbaeva, M.O., "Loading and Unloading Breathing During Exercise: Respiratory Responses and Compensatory Mechanisms," *European Journal of Medical Research*, Vol. 15 (Suppl. 2), 2010, pp. 157-163.
- <sup>37</sup>Molchaski, P., Unterkofler, K., Teschl, G., and Amann, A., "Potential of Volatile Organic Compounds as Markers of Entrapped Humans for Use in Urban Search-and-Rescue Operations," *Trends in Analytical Chemistry*, Vol. 68, May 2015, pp. 88-106.
- <sup>38</sup>Ryder, V. E., "Spacecraft Maximum Allowable Concentrations for Airborne Contaminants," NASA JSC-20584, Sept. 2017.
  <sup>39</sup>Roohi, S.N., Monje, O., Perry, J.L., and Lange, K.E., "Dynamic Modeling of Ammonia Removal with Phosphoric-Acid-Treated Activated Carbon," ICES-2018-319, 48th International Conference on Environmental Systems, Albuquerque, New Mexico, 2018.
- <sup>40</sup>Roohi, S.N., Kayatin, M.J., Perry, J.L., and Lange, K.E., "Dynamic Modeling of Gaseous Multicomponent Trace Contaminant Adsorption," ICES-2019-238, 49<sup>th</sup> International Conference on Environmental Systems, Boston, Massachusetts, 2019.
- <sup>41</sup>Kayatin, M.J., "Chemical Functionalization of Single-Walled Carbon Nanotubes for Compatibilization with Unsaturated Polyester Resin," Ph.D. Dissertation, Chemical Engineering Dept., Auburn Univ., Auburn, AL, 2012.
- <sup>42</sup>Shimanouchi, T., and Shimanouchi, T., "Tables of molecular vibrational frequencies," National Bureau of Standards., Washington, DC, 1980.

<sup>43</sup>Ogata, Y., and Kawasaki, A, "Kinetics of the Condensation of Acetaldehyde with Ammonia," *Tetrahedron*, Vol. 20, No. 4, 1964, pp. 855-860.

<sup>44</sup>Hull, W.E., Sykes, B.D., and Babior, B.M., "Nuclear Magnetic Resonance Proton Study of the Aqueous Chemistry of Acetaldehyde and Ammonia. Formation of 2,4,6-trimethyl-hexahydro-S-triazine," *The Journal of Organic Chemistry*, Vol. 38, No. 17, 1973, pp. 2931-2939.

<sup>45</sup>Duvernay, F., Dufauret, V., Danger, G., Theulé, P., Borget, F., and Chiavassa, T., "Chiral Molecule Formation in Interstellar Ice Analogs: alpha-aminoethanol NH2CH(CH3)OH," *Astronomy & Astrophysics*, Vol. 523, 2010, p. A79.

<sup>46</sup>Vinogradoff, V., Duvernay, F., Farabet, M., Danger, G., Theulé, P., Borget, F., Guillemin, J.C., and Chiavassa, T., "Acetaldehyde Solid State Reactivity at Low Temperature: Formation of the Acetaldehyde Ammonia Trimer," *The Journal of Physical Chemistry A*, Vol. 116, No. 9, 2012, pp. 2225-2233.

<sup>47</sup>Perry, J.L., Abney, M.B, Conrad, R.E., Frederick, K.R., Greenwood, Z.W., Kayatin, M.J., Knox, J.C., Newton, R.L., Parrish, K.J., Takada, K.C., Miller, L.A., Scott, J.P., and Stanley, C.M., "Evaluation of an Atmosphere Revitalization Subsystem for Deep Space Exploration Missions," ICES 2015-107, 45<sup>th</sup> International Conference on Environmental Systems, Bellevue, Washington, 2015.

<sup>48</sup>Kayatin, M.J., and Perry, J.L., "Trace Contaminant Control Design Considerations for Enabling Exploration Missions," ICES 2015-108, 45<sup>th</sup> International Conference on Environmental Systems, Bellevue, Washington, 2015.

<sup>49</sup>Kayatin, M.J., and Perry, J.L., "Evaluation of a Candidate Trace Contaminant Control Subsystem Architecture: The High Velocity, Low Aspect Ratio (HVLA) Adsorption Process," ICES 2017-257, 47<sup>th</sup> International Conference on Environmental Systems, Charleston, South Carolina, 2017.